physica status solidi

pss

www.pss-journals.com

reprint

WILEY-VCH

Phys. Status Solidi C 8, No. 7–8, 2466–2468 (2011) / DOI 10.1002/pssc.201001169

physica status solidi c
www.pss-c.com
current topics in solid state physics

Photovoltaic action from $In_xGa_{1-x}N$ p-n junctions with x > 0.2 grown on silicon

Iulian Gherasoiu[*,1], Lothar A. Reichertz[,1,2], Kin Man Yu[2], Joel W. Ager III[2], Vincent M. Kao[2], and Wladek Walukiewicz[1,2]**

[1] Rose Street Laboratories of Energy, 3701 E University Dr., Phoenix, AZ 85034, USA
[2] Lawrence Berkeley National Laboratory, 1 Cyclotron Rd., Berkeley, CA 94720, USA

Received 15 October 2010, revised 8 February 2011, accepted 15 February 2011
Published online 17 June 2011

Keywords InGaN, semiconductors, hybrid, silicon substrate, solar cell, tandem, thin film

* Corresponding author: e-mail igheraso@yahoo.com, Phone: +01 480 286 5665, Fax: +01 602 437 1864
** e-mail LAReichertz@lbl.gov, Phone: +01 602 561 9000, Fax: +01 602 437 1864

In this paper, we report systematic investigation of the structural and electronic properties of GaN and $In_xGa_{1-x}N$ alloys with x up to 0.31 grown on Si (111) substrate. P-type doping of $In_xGa_{1-x}N$ using Mg has been achieved consistently with magnesium concentrations up to 10^{21} atoms/cm^3. The first results on photovoltaic action in InGaN p-n junctions with ~20% In fraction grown on silicon are also reported. An open circuit voltage (V_{oc}) of almost 1 V was measured under concentrated (20 x sun) AM1.5G condition. The diode shows the onset of a photoresponse at about 2.6 eV. Relatively low shunt and high series resistance are the key factors limiting performance of the InGaN cells with larger In content.

1 Introduction The wide tunability of the band gap of InGaN spanning from 0.65 eV to 3.4 eV opens up new opportunities for the utilization of this alloy system for solar energy conversion devices [1]. Theoretically, the addition of a top cell with a band gap of ~1.8 eV on a Si cell can boost up the thermodynamic efficiency limit from 29% (Si only) to ~42% under 1 sun (AM1.5G) standard illumination [2]. InGaN films with a composition of 45% In are necessary to obtain the required band gap of 1.8 eV. We have found that the conduction band edge (CBE) of $In_{0.45}Ga_{0.55}N$ is aligned with the valence band edge of Si allowing electron and holes to recombine at the n-InGaN/p-Si interface. This unique band alignment enables the design and fabrication of a two-junction InGaN-Si tandem cell with optimum power conversion efficiency and with a natural tunnel junction [3].

Recently, we have demonstrated a GaN/silicon tandem solar cell [4]. This is a major step forward toward the realization of a high efficiency InGaN – Silicon hybrid cell. Although good quality GaN and InN growth on Si substrates has been reported, the growth of $In_xGa_{1-x}N$ films with x>0.1 on silicon substrate is still a challenging task. In this work, we report systematic investigations of the structural and electronic properties of GaN and $In_xGa_{1-x}N$ alloys with x up to 0.31grown on Si (111) substrates, and the first results on photovoltaic action in InGaN p-n junctions on silicon.

2 Experimental Growth was initiated on 4" Si (111) substrates with an AlN/GaN buffer followed by the InGaN layer. Plasma Assisted Molecular Beam Epitaxy (PA-MBE) technique and metal beam modulation have been employed for maintaining a good control over the material stoichiometry.

Rutherford backscattering spectrometry (RBS) was used for the determination of the film composition, thickness and stoichiometry while the crystallinity was evaluated using both ion channelling and high resolution X-ray diffraction (HRXRD). The free electron background concentration was estimated based on the donor density determined from electrochemical capacitance voltage (ECV) measurements.

A set of 5 InGaN samples were grown on GaN buffers with increasing thickness: 30 nm, 90 nm, 190 nm, 410 nm and 600 nm. A description of the growth conditions has been provided in a previous publication [5]. The thickness of the InGaN layers was in the range from 100 nm to 170 nm.

3 Results and discussion The effect of a GaN buffer on the properties of the InGaN layer was investigated. Figure 1 shows plots of the normalized channelling yield (χ) and the residual donor concentration of the InGaN

layers as a function of the GaN intermediate layer thickness. The donor concentrations appear to be in close correlation to the channelling yield data. Relatively large donor concentration (~10^{19} cm^{-3}) is associated with the GaN buffers thickness smaller than 100nm. Transmission electron microscopy (TEM) confirms that this region of the GaN layer is populated by a large number of dislocations [5] that are propagating into the adjacent InGaN layer. As a result donor impurities such as oxygen or silicon are likely to getter and decorate the dislocations. With increasing buffer layer thickness, the dislocations terminate, and for GaN buffers of 190 nm we have obtained InGaN layers with 31 % indium fraction and good crystallinity (538 arcsec) as estimated by the (0002) reflexion of ω-scan.

.

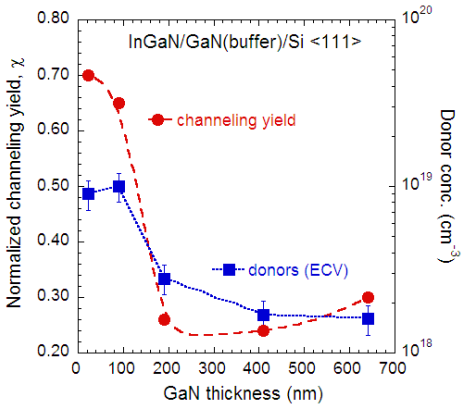

Figure 1 Normalized channelling yield and the residual donor concentration of the InGaN layer as a function of the GaN intermediate layer thickness.

Pseudomorphically grown GaN on AlN is found under compressive stress (c=5.202 Å for 30 nm GaN) and the piezoelectric induced field would bind the negative charges on the GaN side of the heterointerface. Similarly, InGaN layers on GaN should be under compressive stress and negative charges will accumulate on the InGaN side of the heterointerface [6]. With increased thickness the GaN layer relaxes reducing the strain approximately 19 times for GaN with 400 nm thickness (c=5.186 Å), although the stress in the layer remains compressive. The relaxation occurs once the critical thickness of GaN is reached, somewhere around 190 nm in the case of this set of samples, and is not limited to the upper layers of GaN. The relaxation of GaN reduces the interfacial stress, the intensity of the piezoelectric field and therefore the amount of accumulated charge at the GaN/InGaN interface. Donors are charged species that can diffuse under the influence of an electric field and build up gradients within defined volumes, [7]. Figure 2 illustrates the correlation between *c*-lattice spacing, donor concentration in InGaN layers and the thickness of the GaN buffer.

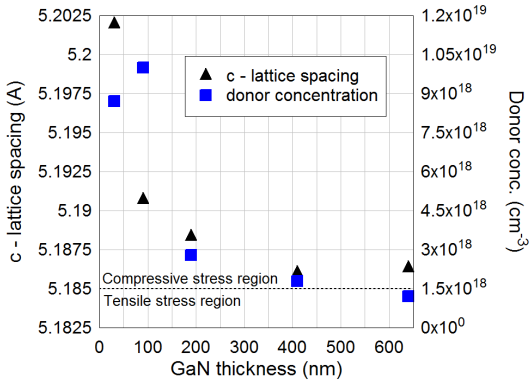

Figure 2 GaN *c*-lattice spacing and residual donor concentration as a function of the GaN layer thickness.

The cell structure of the III–nitride/silicon tandem is illustrated schematically in Fig. 3. The buffer consists of thin AlN followed by 650 nm of undoped GaN. The n-type and p-type InGaN layers were 90 nm and 70 nm thick, respectively. The picture on the right hand side shows a view of the front collector grid of (3x3) mm prototype. Because p-type silicon is used as the substrate in this case, ensuring ohmic contact to the back side of the InGaN stack, the solar cell has only a single p-n junction located within the InGaN layer.

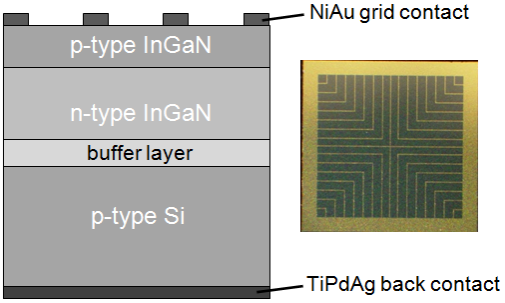

Figure 3 Schematic of the III-nitride/Si solar cell and (3x3) mm prototype.

Magnesium was used for the p-doping of the InGaN while the n-type InGaN is just un-intentionally doped. Secondary ion mass spectrometry (SIMS) measurements indicate a high concentration of magnesium in the top p-type layer (Mg > 10^{21} cm^{-3}). Photolithography and electron beam evaporation were used to deposit defined Ni/Au grid patterns that form the front contact on the top p-type InGaN layer. Electron beam evaporation was also used to deposit Ti/Pd/Ag onto the back side of the Si wafer to form the back ohmic contact. Finally, 1x10^{-4} to 0.1 cm^2 prototype cells were diced from the wafer. The photovoltaic response of the solar cells was measured using 1 sun and concentrated (x20) AM1.5G solar spectrum. Figure 4 shows the I-V curve of a pn-InGaN/p-Si structure for concentrated light conditions. The fraction of indium in this InGaN p-n structure, as determined by RBS, was about

20% which corresponds to a band gap energy of about 2.6 eV. The photoluminescence of the films shown in Fig. 5 exhibits a room temperature peak at ~2.6 eV, in good agreement with the band gap of an InGaN layer with 20% In. The generation of photocurrent for photon energies above 2.6 eV confirms the PV action and separation of charges in the InGaN film. At illumination of 1 sun the open circuit voltage exhibits a low value of $V_{OC} \approx 0.135$ V. With increased concentration (x20) of the solar light the open circuit voltage (V_{OC}) increases to 0.425 V for a (3 x 3) mm device and to 0.975 V when the size of the device is reduced to (0.1 x 0.1) mm. Similarly, the short-circuit current (J_{SC}) increases from 1.82 mA/cm^2 for the larger device to 6.18 mA/cm^2 for the (0.1 x 0.1) mm device. The performance of this cell is limited mainly by the low shunt and high series resistances, indicated by a poor fill factor of 31%, resulting in a power conversion efficiency below 1%. The measured external quantum efficiency is depicted in the insert of Fig. 4 and for this device shows values lower than 10%.

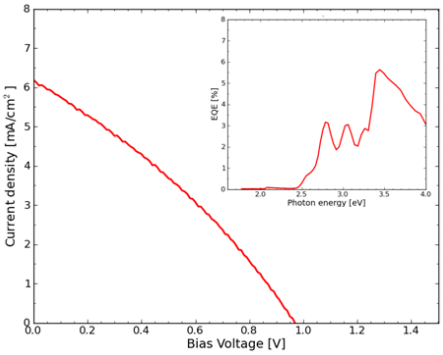

Figure 4 I–V-curve of a 0.1 x 0.1 mm InGaN top cell grown on a silicon wafer illuminated with 20 x sun AM1.5G.

Current leakage across the junction is likely the cause for the low value of the shunt resistance. This conclusion is supported by our observation that selected devices of smaller size exhibit significantly higher open circuit voltages with higher short circuit current densities and better rectification, suggesting that current leakage is related to dislocations spanning across the junction. Band discontinuities created by electrostatic fields within the semiconductor volume and at contact interfaces, on the other hand, could be responsible for the high value of the series resistance. Spontaneous polarization can cause electric fields up to 3 MV/cm in nitride crystals while pseudomorphically grown GaN/InGaN heterointerfaces can exhibit piezoelectric fields of about 2 MV/cm [8]. If these fields are opposed to the built-in electric field across the space charge of the p-n junction, the current collection and the open circuit voltage could be diminished accordingly and the resulting quantum efficiency will be inherently low.

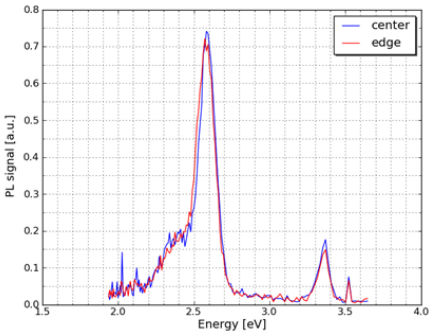

Figure 5 Photoluminescence spectra of InGaN:Mg film grown on Si substrate.

4 Conclusion In conclusion, we have shown the growth of high quality InGaN epitaxial films on Si with In content up to 31%. Prototype InGaN single junction cells were fabricated. A 20% In prototype cell shows a V_{OC} as high as 1 V. Our results strongly suggest that a high efficiency InGaN/Si solar cell can be realized with further reduction of defect density and improvements on the p-type doping of the InGaN materials.

Acknowledgements The work described in this paper on photovoltaic device engineering, materials engineering and epitaxial growth is performed and funded by RoseStreet Labs Energy's line in Phoenix, Arizona. Device processing, characterization and modeling were performed at Lawrence Berkeley National Laboratory (LBNL) and were supported by RSLE through the U.S. Department of Energy, under Contract No. DE-AC02-05CH11231.

References

[1] F. J. Wu, W. Walukiewicz, K. M. Yu, W. Shan, J. W. Ager III, E. E. Haller, H. Lu, W. J. Schaff, W. K. Metzger, and S. Kurtz, J. Appl. Phys. **94**, 6477 (2003).
[2] W. Shockley and H. J. Queisser, J. Appl. Phys. **32**, 510 (1961).
[3] J. W. Ager III, L. A. Reichertz, D. Yamaguchi, L. Hsu, R. E. Jones, K. M. Yu, W. Walukiewicz, and W. J. Schaff, Group III-nitride alloys for multijunction solar cells, Proc. 22nd European PV Solar Energy Conference and Exhibition, Milan, Italy (2007).
[4] L. A. Reichertz, I. Gherasoiu, K. M. Yu, V. M. Kao, W. Walukiewicz, and J. W. Ager III, Appl. Phys. Express **2**, 122202 (2009).
[5] I. Gherasoiu, K. M. Yu, L. A. Reichertz, V. M. Kao, M. Hawkridge, J. W. Ager III, and W. Walukiewicz, Phys. Status Solidi B **247**(7), 1747 (2010).
[6] O. Ambacher, J. Smart, J. R. Shealy, N. G. Weimann, K. Chu, M. Murphy, R. Dimitrov, L. Wittmer, M. Stutzmann, W. Rieger, and J. Hilsenbeck, J. Appl. Phys. **85**(6), 15 (1999).
[7] P. J. Anthony, Solid-State Electron. **25**(12), 1171 (1982).
[8] A. Hangleiter, J. S. Im, H. Kollmer, S. Heppel, J. Off, and F. Scholz, MRS Internet J. Nitride Semicond. Res. **3**, 15 (1998).

